



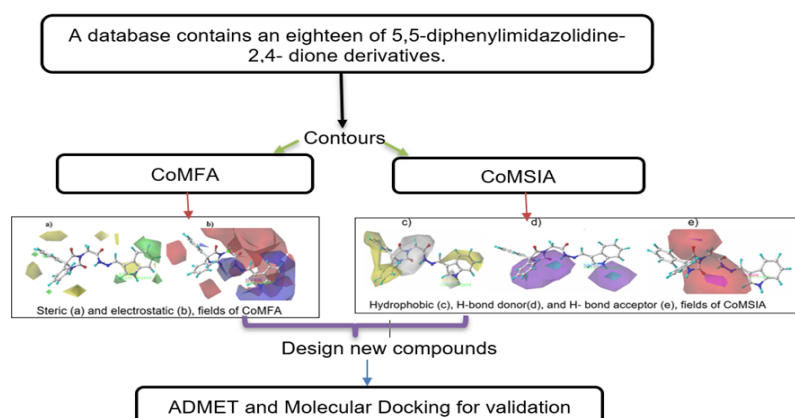
Full Paper | <http://dx.doi.org/10.17807/orbital.v14i1.1659>

3D-QSAR, ADMET and Docking Studies for Design New 5,5-Diphenylimidazolidine-2,4-dione Derivatives Agents Against Cervical Cancer

Reda EL-Mernissi ^a, Khalil EL Khatabi ^a, Ayoub Khaldan ^a, Soukaina Bouamrane ^a, Larbi ELMchichi ^a, Mohammed Aziz Ajana * ^a, Tahar Lakhlifi ^a and Mohammed Bouachrine ^{a,b}

Cancer is one of the world's causes of death, which requires the discovery of new molecules likely to become anticancer drugs. In this study, a three-dimensional quantitative structure-activity relationship is employed to study eighteen compounds of 5,5-diphenylimidazolidine-2,4-dione derivatives against cancer cell lines HeLa, their pIC₅₀ varied from 3.62 to 5.00. In addition, the 3D-QSAR model was defined on the basis of Comparative Molecular Field Analysis (CoMFA) and Comparative Molecular Similarity Indices (CoMSIA) analysis, the model achieved strong predictability with the model CoMFA is ($Q^2 = 0.70$; $R^2 = 0.94$; $r^2_{\text{test}} = 0.96$) and the best one on CoMSIA ($Q^2 = 0.73$; $R^2 = 0.97$; $r^2_{\text{test}} = 0.98$), respectively. We have proposed four compounds with highly potent anticancer predicted activities, based on successful results obtained by the contour maps formed by the method model. Furthermore, the ADMET properties of these newly designed compounds were in silico evaluated, among which two derivatives have respected these properties. These compounds were further evaluated by molecular docking, showing that two molecules T2 and T4 exhibit favorable interactions with the targeted receptor and a high total score. These findings may afford valuable more information to design compounds anticancer activity against Hela cells.

Graphical abstract



Keywords

3D-QSAR
5,5-diphenylimidazolidine-2,4-dione
ADMET
Cancer
Molecular docking

Article history

Received 19 August 2021
Accepted 27 January 2022
Available online 25 March 2022

Handling Editor: Arlan Gonçalves

1. Introduction

Cancer is amongst the most prevalent diseases in the world, there are more than a hundred distinct forms of cancer, it can affect every other organ in the human body, the most

common cancers in the world are breast cancer, prostate cancer lung cancer, and cancer cell lines (HeLa, A549...). The most popular malignancy of woman organs is cervical cancer,

^a Faculty of Science, University Moulay Ismail, MCNSL, BP 11201-Zitoune.50000. Meknes, Morocco. ^b EST Khenifra, Sultan Moulay Sliman University, Benimellal, Morocco. Corresponding author. E-mail: a.ajanamohammed@fs.umi.ac.ma

a common way of treating advanced cervical cancer is platinum-based chemotherapy and radiotherapy. The researchers test the therapeutic efficacy of anti-cancer agents in laboratories by using the human cancer-derived cell lines [1], the first line of cancer developed was HeLa, it emerged in 1951 from Henrietta Lacks taken of cervical cancer cells [2], the cytogenetic studies showed that many cancer cell lines used only to model different types of cancers were originally derived from the cervical cancer line HeLa [3,5]. The treatment for this cancer is consuming almonds, seeds of apricots, and apples, as they contain amygdalin [6,8], cyanide toxicity decreased the use of amygdalin as an anticancer agent [9,11]. This research aims to design new against cancer cell lines HeLa. We have used eighteen compounds of 5,5-diphenylimidazolidine-2,4- dione derivatives against cancer. The fight against cancer is progressing in all areas, which have the path the way to the three-dimensional quantitative structure-activity relationship (3D-QSAR) to be used to design new effective anticancer compounds, through the methods of comparative molecular field analysis (CoMFA) and comparative molecular similarity indices (CoMSIA). To determine pharmacokinetic properties and toxicity, the ADMET online was used. To discover the binding modes of compounds with the active site of EGFR tyrosine kinase protein (PDB code: 2ITY), molecular docking was performed by using surflex-docking, and the reliability of the proposed compounds was achieved.

2. Results and Discussion

2.1 Molecular alignment

Alignment is an important step in 3D-QSAR, this step requires the use of sybyl. the core used is 2-(2,5-dioxo-4,4-diphenylimidazolidin-1-yl) acetaldehyde and the template is compound 12, for this step, the result is shown in Figure 1.

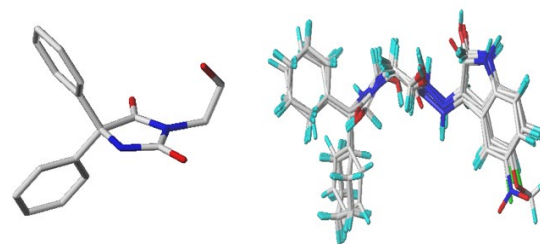


Figure 1. 3D structure of the core (left) and aligned compounds (right).

2.2 CoMFA and CoMSIA studies

3D-QSAR was built on the CoMFA and CoMSIA contours, the total number of molecules is divided into two classes, training and test set composed of 14 and 4 compounds, respectively. The best results found in the CoMFA model are good cross-validated correlation coefficient with $Q^2 = 0.70$, non-cross-validated correlation coefficient $R^2 = 0.94$, Standard error of the estimate $Scv = 0.11$, a value of external validation $rext^2 = 0.96$, and F-value with 55.51, with 3 components. The percentage of participation steric and electrostatic fields is 79% and 21% respectively.

The result of CoMSIA model showed an acceptable values of cross-validated correlation coefficient with $Q^2 = 0.73$, non-cross-validated correlation coefficient $R^2 = 0.97$, Standard error of the estimate $Scv = 0.08$, a value of external validation $rext^2 = 0.98$, and F-value with 87.86, with 3 components. The percentage participation of steric, electrostatic, hydrogen bond acceptor, hydrogen bond donor, and hydrophobic fields were 18%, 13%, 6%, 40%, and 32%, respectively. The statistical parameters associated with the CoMFA and CoMSIA models are given in Table 1. Table 2 shows the predicted and observed pIC50 values of the training set and test set.

Table 1. The PLS statistical results of methods models.

Models	Q ²	R ²	SCV	F	N	rext ²	Fraction				
							Steric	Elec	Acc	Don	Hyd
CoMFA	0.70	0.94	0.11	55.51	3	0.96	0.79	0.21	-	-	-
CoMSIA	0.73	0.97	0.08	87.86	3	0.98	0.18	0.13	0.16	0.40	0.32

Table 2. Observed and predicted activities of 5,5-diphenylimidazolidine-2,4- dione derivatives.

N	pIC ₅₀ (M)	CoMFA	CoMSIA	N	pIC ₅₀ (M)	CoMFA	CoMSIA
		Predicted	Predicted			Predicted	Predicted
1	3.62	3.52	3.50	10	4.28	4.22	4.23
2	3.63	3.48	3.47	11	4.41	4.45	4.45
3*	3.77	3.97	3.77	12	5.00	4.83	4.79
4	3.91	3.98	4.00	13	4.52	4.51	4.51
5	3.77	3.93	3.96	14*	4.28	4.28	4.20
6	3.91	4.03	4.06	15	4.73	4.64	4.64
7	4.22	4.17	4.20	16	4.54	4.58	4.58
8*	4.30	4.18	4.15	17	4.52	4.57	4.57
9	3.95	4.04	4.05	18*	3.93	4.17	4.16

* test set

The experimental and predicted values are closer, so our program is accurate. The relationship between observed and expected activity data for CoMFA model and CoMSIA model is shown in Figure 2.

The values of R^2 tend towards 1, and the cloud of points narrows around the regression line, this means that the model

used is reliable.

2.3 Y-randomization

A technique Y-randomization [23] was used to verify the correlation between the structures of the compounds and pIC₅₀, this method is based on randomly change the pIC₅₀

between compounds. Table 3 displays the results produced. We obtained a new model with lower Q² and R² values after

every randomization, which indicates that the correlation is not random.

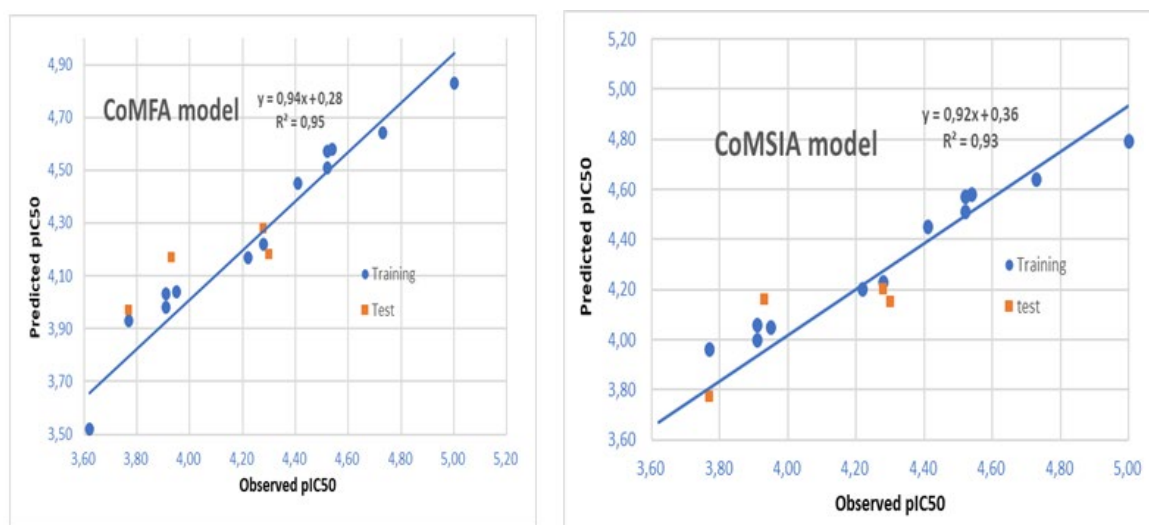


Figure 2. Experimental versus expected pIC₅₀ values scatter plot (test set represented as red Square).

Table 3. Q² and R² values obtained after several Y – randomization tests.

Iteration	CoMFA		CoMSIA	
	Q ²	R ²	Q ²	R ²
1	-0.236	0.255	-0.235	0.277
2	-0.200	0.213	-0.143	0.443
3	-0.217	0.443	-0.320	0.393
4	-0.091	0.235	-0.111	0.433
5	-0.176	0.200	-0.151	0.335
6	-0.340	0.351	-0.237	0.363

The values obtained suggest that there is no random correlation between the structures of the compounds and their pIC₅₀.

2.4 CoMFA and CoMSIA contour maps

The CoMFA and CoMSIA contours are needed to increase the activity of the compounds using a 3D-QSAR study. The compound 12 template was used to collect further details on the decrease or increase activity. The default 20% and 80% level contributions for unflavored and favored regions were represented by both models.

2.4.1 CoMFA contour maps

Steric and electrostatic fields have percentages of 79% and 21% in steric areas, respectively, the steric (a) and electrostatic (b) fields of the CoMFA and CoMSIA models are presented in Figure 3.

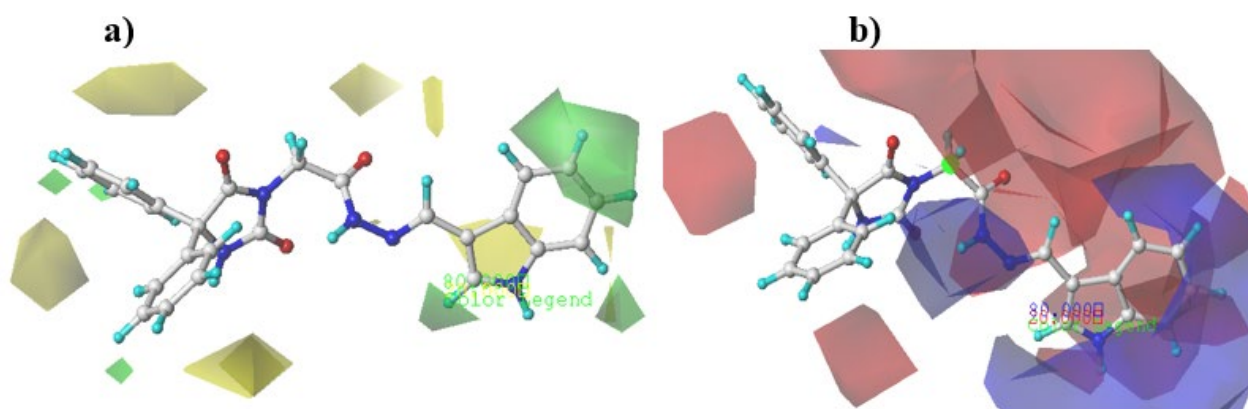


Figure 3. Steric (a) and electrostatic (b) contours maps of the CoMFA and CoMSIA analysis with 2 Å grid spacing in combination.

In Figure 3a: The green contours designate a large group that prefers activity, while yellow contours indicate a large group that opposes activity. The green color near the 2,5,6 and 7 positions in the R1 (indole) substituents, could explain why compound 16 (pIC₅₀=4.54) actual activity is higher than that of compound 14 (pIC₅₀=4.28).

In Figure 3b: The red colors appear closer to position 2 in the indole, indicate regions where groups with positive

charges decrease activity, but the blue colors located near all positions (except position 2) of indole which belongs to R1, the show of the positive charge in this position increases the activity, this explains the higher activity of some compounds 15 (pIC₅₀=4.73) and 16 (pIC₅₀=4.54).

2.4.2 CoMSIA contour maps

The hydrophobic, H-bond donor and H-bond acceptor

fields of CoMSIA are shown in Figures 4c, 4d, 4e, respectively.

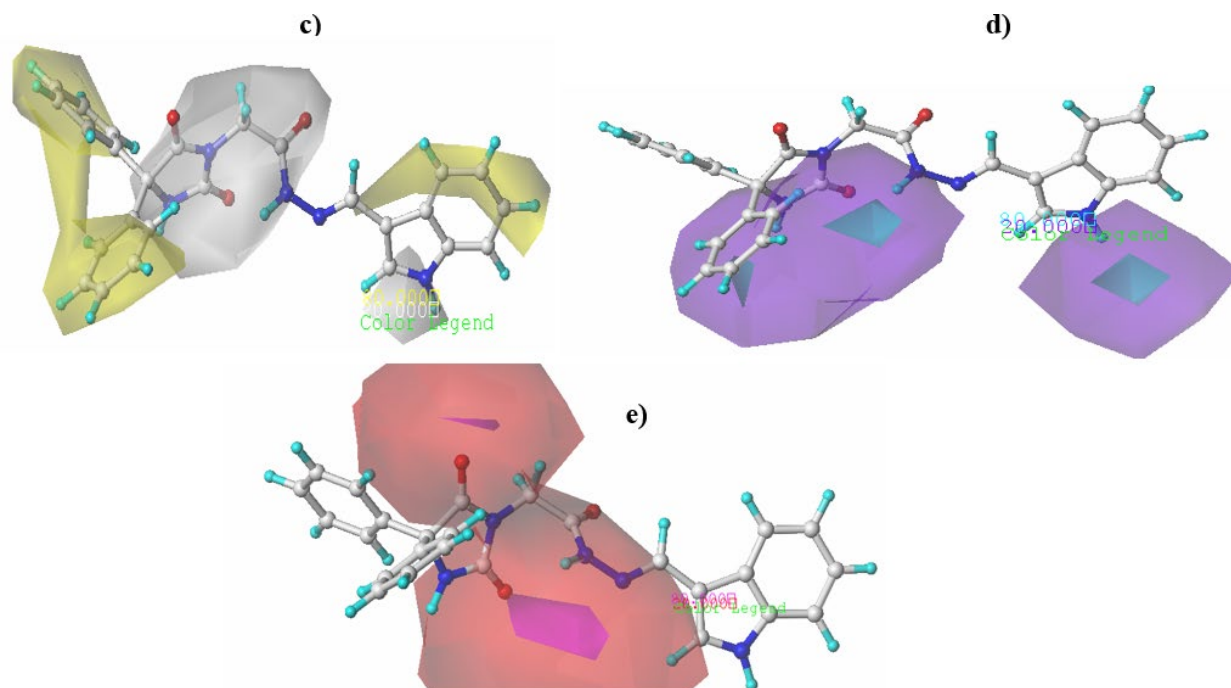


Figure 4. Hydrophobic (c), H-bond donor(d), and H- bond acceptor (e) contours maps of the CoMSIA.

The fields that have a higher participation percentage are hydrophobic and H-bond donor, with values 32% and 40% respectively, in to increase the activity of the compounds we based only on these contours.

In Figure 4e: The white color around the indole location of 1,2 suggests that hydrophilic groups are preferred to increase activity. In comparison, the yellow contours around the positions of 3,4,5, and 6 suggest that hydrophilic groups are not preferred for increasing activity. This explains the higher activity of compound 7 (pIC50 = 4.22) compared to compound 6 (pIC50 = 3.91).

In Figure 4d: The cyan contours around the indole location

of 1 suggests that H-bond donor groups are preferred to increase activity. The yellow contours around the positions of 2 and 7 suggest that H-bond donor groups are not preferred for increasing activity. This explains the higher activity of compound 12 (pIC50 = 5.00) compared to the activity values of other compounds.

2.5 New designed compounds

Four compounds were designed using the template compound 12 (pIC50= 5.00) and with the positive results found in CoMFA and CoMSIA models. The structure and pIC50 values of the predicted compounds are presented in Table 4.

Table 4. The structures of new molecules and their pIC50 values.

N°	R	Predicted (pIC50)		N°	R	Predicted (pIC50)	
		CoMFA	CoMSIA			CoMFA	CoMSIA
12		5.00	5.16	T3		5.14	5.29
T1		5.20	5.45	T4		5.30	5.49
T2		5.19	5.32				

All predicted compounds have higher pIC_{50} values compared to the value of compound 12.

2.6 ADMET prediction

Characterization of absorption, distribution, metabolism,

and excretion (ADMET) is an essential step in predicting the properties of drugs, these features were obtained by using Swissadme and pKSM online tool successively. Table 5 shows the ADMET prediction of compounds 12 and the proposed compounds (T1–T4).

Table 5. ADMET prediction of newly designed inhibitors.

N°	Absorption		Distribution		Metabolism							Excretion	Toxicity
	Water Solubility (log mol/L)	Intestine Absorption (human) (% absorbed)	Volume of distribution (logL/Kg)	Blood-brain barrier permeability (log BB)	Substrate		Inhibition					Total Clearance (log mL/min/Kg)	Toxicity Ames (Yes/No)
					CYP								
					2D6	3A4	1A2	2C19	2C9	2D6	3A4		
(Yes/No)										(log mL/min/Kg)	(Yes/No)		
T1	-3.59	77.41	0.17	-1.31	No	Yes	No	Yes	Yes	No	Yes	0.33	No
T2	-3.51	85.42	0.67	-1.90	No	Yes	No	No	No	No	Yes	0.52	No
T3	-3.19	70.60	0.24	-1.33	No	Yes	No	No	No	No	Yes	0.76	No
T4	-3.71	71.84	0.56	-1.56	No	Yes	No	Yes	Yes	No	Yes	0.93	No

The poor absorption is linked to the poor solubility of the drugs in water, our objective is to eliminate the compounds which soluble a little in water, i.e., which have water solubility values <-4 , in this table all compounds respect this value. In addition, a drug has a good absorbance if their values exceed 30%, all compounds have values greater than 60%, this shows a good absorption in the human intestine. The predicted distribution (VDss) and blood-brain permeability (log BB), the values are accepted if values (VDss) > 0.45 and (log BB) <-1 , respectively, the results obtained show that all compounds have (log BB) <-1 , but only compounds T2 and T4 have (VDss) > 0.45 . In Metabolism, 3A4 is responsible for the metabolism, all predicted compounds are substrates and inhibitors for 3A4, but on the contrary for 2D6 are not. In Excretion, all compounds are non-toxic and have good total clearance values, except compound T1 has poor clearance. Therefore, compounds T2 and T4 are important compounds against cancer.

2.7 Docking results

To examine and see the 2D view binding modes of the proposed (T2 and T4) and 12 compounds with the active site of EGFR tyrosine kinase protein (PDB code: 2ITY), we used molecular docking, in which the results obtained are shown in Table 6.

All compounds have conventional hydrogen bond interactions, which increases the stability of these complexes. Moreover, only compound 12 has unfavorable donor-donor interaction, the stability of this complex is decreased. To continue the comparison of the stability of these complexes, Table 7 shows the types of interactions and total scoring.

The most stable compounds are T2 and T4 because have higher values in total scoring (5.02 and 5.00), respectively, also in types of interactions H-bond, and they have not any interaction unfavorable donor-donor types, which we can conclude that these compounds improve the anticancer activity against Hela cells.

Table 7. Types of interaction and total scoring

N°	Types of interactions		Total scoring
	Hydrogen Bond	Unfavorable Donor-Donor	
12	Leu 788.	Leu 745.	4.40
T2	Pro 794, Met 793.	-	5.02
T4	Gln 791, Cys 797.	-	5.00

3. Material and Methods

3D-QSAR modeling was executed on a set of 18 substituted 5,5-diphenylimidazolidine-2,4-dione anticancer derivatives which were taken from the literature [12], the data set was divided into two sets, 14 compounds were selected as the training set and the rest 4 were selected as a test set, these compounds have a star (*), the random choice test set to determine the performance of a model produced. The CoMFA and CoMSIA contours are important to build 3D-QSAR and analyze physical-chemical properties. Originally IC_{50} value was observed by unit (μM) and translated into pIC_{50} (M) as ($pIC_{50} = \text{Log } 1 / IC_{50}$), Figure 5 shows the molecular structure of the substances studied, and the Table 8 shows the different structures for the test and training substances and their biological activities pIC_{50} .

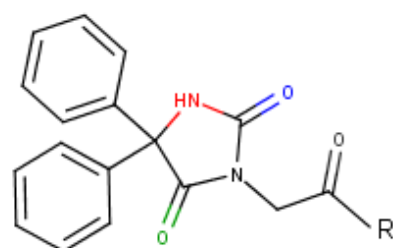


Figure 5. Structure of the studied compounds.

Table 6. 2D View of the binding conformation of the proposed (T2 and T4) and 12 compounds with the active site of EGFR tyrosine kinase protein.

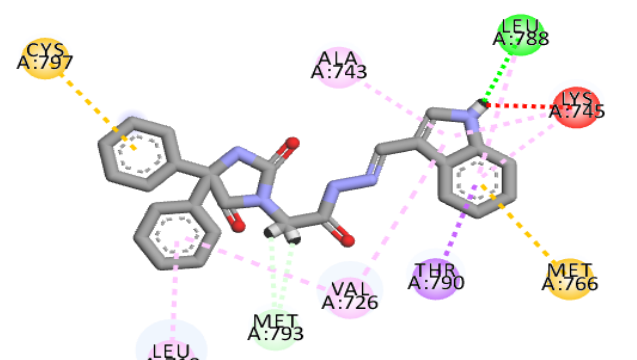
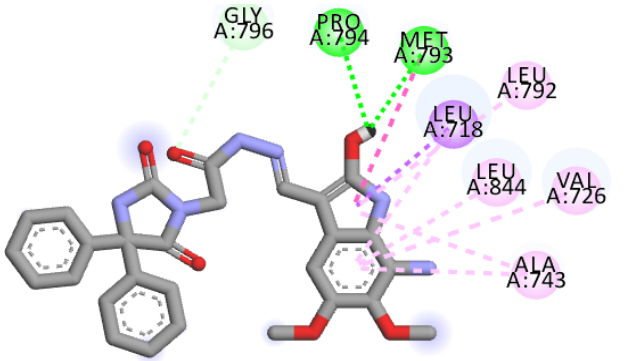
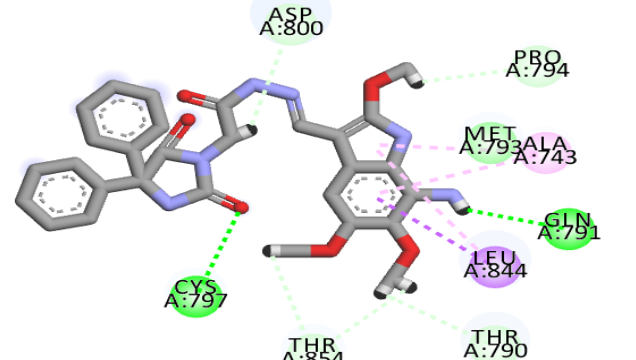
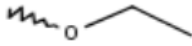
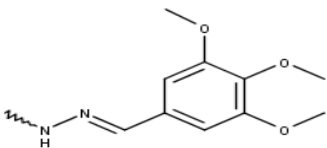
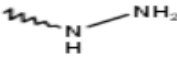
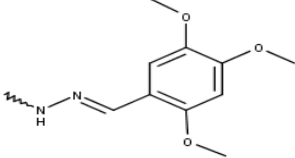
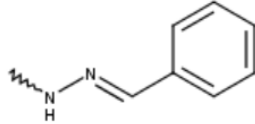
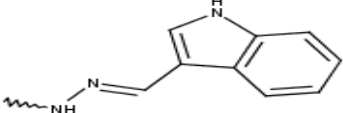
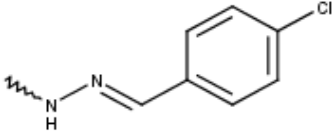
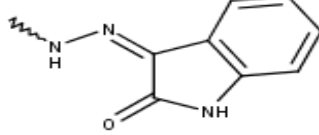
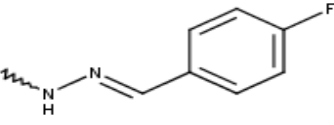
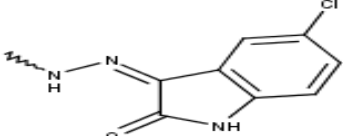
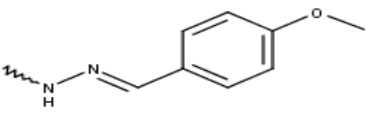
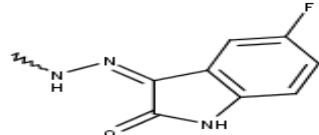
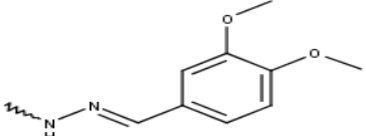
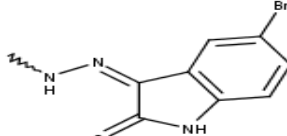
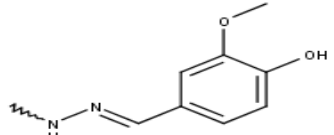
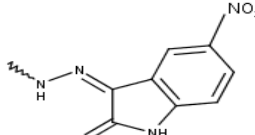
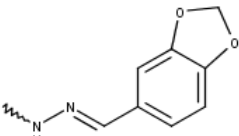
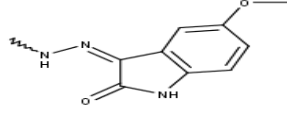
N°	2D View
12	 <p>Interactions</p> <ul style="list-style-type: none"> ■ Conventional Hydrogen Bond ■ Carbon Hydrogen Bond ■ Unfavorable Donor-Donor ■ Pi-Sigma ■ Pi-Sulfur ■ Pi-Alkyl
T ₂	 <p>Interactions</p> <ul style="list-style-type: none"> ■ Conventional Hydrogen Bond ■ Carbon Hydrogen Bond ■ Pi-Sigma ■ Amide-Pi Stacked ■ Pi-Alkyl
T ₄	 <p>Interactions</p> <ul style="list-style-type: none"> ■ van der Waals ■ Conventional Hydrogen Bond ■ Carbon Hydrogen Bond ■ Pi-Sigma ■ Pi-Alkyl

Table 8. The structure and activities of studied compounds.

N°	R ₁	pIC ₅₀ (M)	N	R ₁	pIC ₅₀ (M)
1		3.62	10		4.28
2		3.63	11		4.41
3*		3.77	12		5.00
4		3.91	13		4.52
5		3.77	14*		4.28
6		3.91	15		4.73
7		4.22	16		4.54
8*		4.30	17		4.52
9		3.95	18*		3.93

3.1. Minimization and alignment

The consistency of molecular alignment was identified as an important factor for the modifiability and analytical active power of CoMFA and CoMSIA models, compound 12 is the most active in our database, it's a template of all compounds (Figure 6). The sybyl software [13] is used to minimize compounds with Gasteiger-Huckel charge [14].

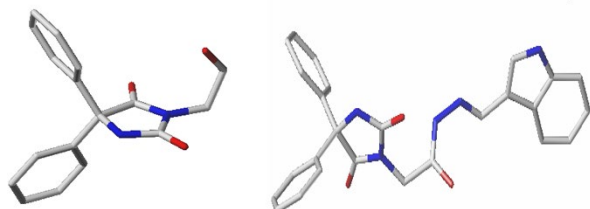


Figure 6. 3D structure of the core (left) and the template (right).

3.2 CoMFA and CoMSIA studies

The CoMFA [15] and CoMSIA [16] were used to create 3D-QSAR, and both contours were built using Sybyl-x 2.1 (Tripos, Inc, USA). The electrostatic and steric fields of CoMFA was produced at every crystal structure point of the grid box of 2.0 Å. Threshold values of 30 kcal/mol. In addition to the electrostatic and steric, CoMSIA contour also represents the Electrostatic, H bond donor and H bond acceptor fields. The regression technique of partial least square (PLS) [17] was used to performing our study of CoMFA and CoMSIA. The leave-One-Out (LOO) cross-validation method was performed in the first PLS analysis, it is used to determine the coefficient of cross-validation correlation (Q^2), non-cross validated correlation coefficient (R^2), and the optimal number of components (N), value F Fischer test and lowest value of the standard error of estimates (SEE). Furthermore, the external validation r^2_{ext} was used as a test set to estimate the predictive model capable of the obtained models by using 4 molecules. If the values $Q^2 > 0.50$, $R^2 > 0.60$, the optimum number of component values and the standard error estimate (SEE) are low, it is best to use this model.

3.3 Y-randomization

The construction of a new QSAR model is carried out with the change of the pIC50 in a random way, the random correlation between the structures and their pIC50, the values found of the Q^2 and R^2 are low compared to the models of origin, this step named a Y-Randomization [18].

3.4 Model acceptability criteria

Researchers Golbraikh Alexander and Tropsha determine the best models such as Q^2 value > 0.5 , $R^2 > 0.6$, and $r^2_{test} > 0.6$, this type of model is accepted [19].

3.5 ADMET Prediction

Pharmacokinetics include absorption of the molecule, distribution in the body, elimination including biotransformation or Metabolism, Excretion, and toxic (ADMET). This study used swissadmet web server [20] for predicting the ADMET properties. ADMET prediction is an essential part of discovery process, where the precise results from help to identify the best drug candidates.

3.6 Molecular Docking

To confirm the 3D-QSAR, we have analyzed the binding interactions between The EGFR tyrosine kinase protein (PDB code: 2ITY) obtained from the Protein databank PDB site (www.rcsb.org) and ligands. The surflex-Dock module of Sybyl was used for molecular docking studies, and the total score. The protein and ligands preparation steps for the docking protocol were performed in pymol [21]. Consequently, the results were observed by using Discovery Studio 2016 [22].

4. Conclusions

In this study, series of eighteen 5,5-diphenylimidazolidine-2,4-dione derivatives anticancer activity against Hela cells, were studied using 3D-QSAR through CoMFA and CoMSIA models, showing efficient predictability and stability. The contour maps generated from 3D-QSAR studies constitute the major structural features required in terms of favorable and unfavorable replacements which could influence the activity. Consequently, based on the useful guidelines developed by 3D-QSAR, news 5,5-diphenylimidazolidine-2,4-dione derivatives were proposed with high activity against cancer. The results of the ADMET, molecular docking, and total scoring studies show that the compounds T2 and T4 were demonstrated as most active anticancer inhibitors.

Acknowledgments

The "Association Marocaine des Chimistes Théoriciens" (AMCT) deserves special appreciation for its valuable assistance.

Author Contributions

Reda EL-Mernissi: Data curation, Formal analysis, Investigation, Methodology, Resources, Software, Writing - original draft. Khalil EL Khatabi: Investigation, Resources, Software. Ayoub Khaldan: Investigation, Methodology. Soukaina Bouamrane: Investigation. Larbi EIMchichi: Investigation, Methodology. Mohammed Aziz Ajana: Conceptualization, Project administration, Supervision, Validation, Visualization. Tahar Lakhli: Conceptualization, Project administration, Supervision, Validation, Visualization. Mohammed Bouachrine: Conceptualization, Methodology, Project administration, Supervision, Validation, Visualization.

References and Notes

- [1] Sharma, S. V.; Haber, D. A.; Settleman, J. *Nat. Rev. Cancer* **2010**, *10*, 241. [\[Crossref\]](#)
- [2] Scherer, W. F.; Syverton, J. T.; Gey, G. O. *J. Exp. Med.* **1953**, *97*, 695. [\[Crossref\]](#)
- [3] Nelson-Rees, W. A. *Prog. Clin. Biol. Res.* **1978**, *26*, 25. [\[Link\]](#)
- [4] Nelson-Rees, W. A.; Flandermeyer, R. R. *Science* **1977**, *195*, 1343. [\[Link\]](#)
- [5] Nelson-Rees, W. A.; Flandermeyer, R. R.; Hawthorne, P. K. *Science* **1974**, *184*, 1093. [\[Crossref\]](#)
- [6] Chang, H. K.; Shin, M. S.; Yang, H. Y.; Lee, J. W.; Kim, Y. S.; Lee, M. H.; Kim, J.; Kim, K. H.; Kim, C. J. *Biol. Pharm. Bull.* **2006**, *29*, 1597. [\[Crossref\]](#)
- [7] Park, H. J.; Yoon, S. H.; Han, L. S.; Zheng, L. T.; Jung, K.

- H.; Uhm, Y. K.; Lee, J. H.; Jeong, J. S.; Joo, W. S.; Yim, S. V.; Chung, J. H.; Hong, S. P. *World J. Gastroenterol.* **2005**, 11, 5156. [\[Crossref\]](#)
- [8] Fukuda, T.; Ito, H.; Mukainaka, T.; Tokuda, H.; Nishino, H.; Yoshida, T. *Biol. Pharm. Bull.* **2003**, 26, 271. [\[Crossref\]](#)
- [9] Flora, K. P.; Cradock, J. C.; Ames, M. M. *Commun. Chem. Pathol. Pharmacol.* **1978**, 20, 367. [\[Link\]](#)
- [10] Khandekar, J. D.; Edelman, H. *JAMA* **1979**, 242, 169. [\[Crossref\]](#)
- [11] Moertel, C. G.; Ames, M. M.; Kovach, J. S.; Moyer, T. P.; Rubin, J. R.; Tinker, J. H. *JAMA* **1981**, 245, 591. [\[Link\]](#)
- [12] Alkahtani, H. M.; Alanazi, M. M.; Aleanizy, F. S.; Alqahtani, F. Y.; Alhoshani, A.; Alanazi, F. E.; Almehizia, A. A.; Abdalla, A. N.; Alanazi, M. G.; El-Azab, A. S.; Abdel-Aziz, A. A.-M. *Saudi Pharm. J.* **2019**, 27, 682. [\[Crossref\]](#)
- [13] Louis, MO. Tripos Inc., St, USA, no. SYBYL-X 2.0, (n.d). [\[Link\]](#)
- [14] Purcell, W. P.; Singer, J. A. *J. Chem. Eng. Data* **1967**, 12, 235. [\[Crossref\]](#)
- [15] Cramer, R. D.; Patterson, D. E.; Bunce, J. D. *J. Am. Chem. Soc.* **1988**, 110, 5959. [\[Crossref\]](#)
- [16] Klebe, G.; Abraham, U.; Mietzner, T. *J. Med. Chem.* **1994**, 37, 4130. [\[Crossref\]](#)
- [17] Bush, B. L.; Nachbar, R. B. *J. Comput. Aided Mol.* **1993**, 7, 587. [\[Crossref\]](#)
- [18] El Khatabi, K.; Aanouz, I.; El-mernissi, R.; Khaldan, A.; Ajana, M. A.; Bouachrine, M.; Lakhlifi, T. *Orbital: Electron. J. Chem.* **2020**, 12, 172. [\[Crossref\]](#)
- [19] Tropsha, A.; Gramatica, P.; Gombar, V. K. *QSAR Comb. Sci.* **2003**, 22, 69. [\[Crossref\]](#)
- [20] Daina, A.; Michielin, O.; Zoete, V. *Sci. Rep.* **2016**, 7, 1. [\[Crossref\]](#)
- [21] DeLano, W. L. *CCP4 Newsl. Protein Crystallogr.* **2002**, 40, 82.

How to cite this article

El-Mernissi, R.; Khatabi, K. E.; Khaldan, A.; Bouamrane, S.; ElMchichi, L.; Ajana, M. A.; Lakhlifi, T.; Bouachrine, M. *Orbital: Electron. J. Chem.* **2022**, 14, 24. DOI: <http://dx.doi.org/10.17807/orbital.v14i1.1659>